

The center of mass motion of short-range correlated nucleon pairs studied via the $A(e, e'pp)$ reaction

E. O. Cohen,¹ O. Hen,^{2,*} E. Piasetzky,¹ L.B. Weinstein,³ M. Duer,¹ A. Schmidt,² I. Korover,¹ H. Hakobyan,⁴ S. Adhikari,¹⁷ Z. Akbar,¹⁸ M.J. Amarian,³ H. Avakian,³⁸ J. Ball,¹¹ L. Barion,¹⁹ M. Battaglieri,²¹ A. Beck,^{2,†} I. Bedlinskiy,²⁵ A.S. Biselli,^{15,9} S. Boiarinov,³⁸ W. Briscoe,⁴⁵ V.D. Burkert,³⁸ F. Cao,¹³ D.S. Carman,³⁸ A. Celentano,²¹ G. Charles,²⁴ Pierre Chatagnon,²⁴ T. Chetry,³² G. Ciullo,^{19,16} Brandon A. Clary,¹³ M. Contalbrigo,¹⁹ V. Crede,¹⁸ R. Cruz Torres,² A. D'Angelo,^{22,34} N. Dashyan,⁴⁴ R. De Vita,²¹ E. De Sanctis,²⁰ M. Defurne,¹¹ A. Deur,³⁸ S. Diehl,¹³ C. Djalali,³⁶ M. Duer,¹ R. Dupre,²⁴ H. Egiyan,³⁸ Mathieu Ehrhart,²⁴ A. El Alaoui,⁴ L. El Fassi,²⁸ P. Eugenio,¹⁸ G. Fedotov,³² R. Fersch,^{12,43} A. Filippi,²³ Y. Ghandilyan,⁴⁴ K.L. Giovanetti,²⁶ F.X. Girod,³⁸ E. Golovatch,³⁵ R.W. Gothe,³⁶ K.A. Griffioen,⁴³ K. Hafidi,^{5,44} N. Harrison,³⁸ F. Hauenstein,³ D. Heddle,^{12,38} K. Hicks,³² M. Holtrop,²⁹ D.G. Ireland,⁴⁰ B.S. Ishkhanov,³⁵ E.L. Isupov,³⁵ D. Jenkins,⁴¹ H.S. Jo,²⁷ S. Johnston,⁵ M.L. Kabir,²⁸ D. Keller,⁴² G. Khachatryan,⁴⁴ M. Khachatryan,³ M. Khandaker,^{31,‡} A. Kim,¹³ W. Kim,²⁷ A. Klein,³ F.J. Klein,¹⁰ I. Korover,³⁰ V. Kubarovskiy,^{38,33} S.E. Kuhn,³ L. Lanza,²² P. Lenisa,¹⁹ K. Livingston,⁴⁰ I. J. D. MacGregor,⁴⁰ D. Marchand,²⁴ B. McKinnon,⁴⁰ S. Mey-Tal Beck,^{2,†} C.A. Meyer,⁹ M. Mirazita,²⁰ V. Mokeev,^{38,35} R.A. Montgomery,⁴⁰ A Movsisyan,¹⁹ C. Munoz Camacho,²⁴ B. Mustapha,⁵ P. Nadel-Turonski,³⁸ S. Niccolai,²⁴ G. Niculescu,²⁶ M. Osipenko,²¹ A.I. Ostrovidov,¹⁸ M. Paolone,³⁷ R. Paremuzyan,²⁹ E. Pasyuk,^{38,6} O. Pogorelko,²⁵ J.W. Price,⁷ Y. Prok,^{3,42} D. Protopopescu,⁴⁰ M. Ripani,²¹ D. Riser,¹³ A. Rizzo,^{22,34} G. Rosner,⁴⁰ P. Rossi,^{38,20} F. Sabatié,¹¹ B.A. Schmookler,² R.A. Schumacher,⁹ Y.G. Sharabian,³⁸ D. Sokhan,⁴⁰ N. Sparveris,³⁷ S. Stepanyan,³⁸ S. Strauch,³⁶ M. Taiuti,²¹ J.A. Tan,²⁷ M. Ungaro,^{38,33} H. Voskanyan,⁴⁴ E. Voutier,²⁴ R. Wang,²⁴ D.P. Watts,³⁹ X. Wei,³⁸ M.H. Wood,^{8,36} N. Zachariou,³⁹ J. Zhang,⁴² X. Zheng,⁴² and Z.W. Zhao¹⁴

(The CLAS Collaboration)

¹School of Physics and Astronomy, Tel Aviv University, Tel Aviv 69978, Israel

²Massachusetts Institute of Technology, Cambridge, Massachusetts 02139, USA

³Old Dominion University, Norfolk, Virginia 23529

⁴Universidad Técnica Federico Santa María, Casilla 110-V Valparaíso, Chile

⁵Argonne National Laboratory, Argonne, Illinois 60439

⁶Arizona State University, Tempe, Arizona 85287-1504

⁷California State University, Dominguez Hills, Carson, CA 90747

⁸Canisius College, Buffalo, NY

⁹Carnegie Mellon University, Pittsburgh, Pennsylvania 15213

¹⁰Catholic University of America, Washington, D.C. 20064

¹¹IRFU, CEA, Université Paris-Saclay, F-91191 Gif-sur-Yvette, France

¹²Christopher Newport University, Newport News, Virginia 23606

¹³University of Connecticut, Storrs, Connecticut 06269

¹⁴Duke University, Durham, North Carolina 27708-0305

¹⁵Fairfield University, Fairfield CT 06824

¹⁶Università di Ferrara, 44121 Ferrara, Italy

¹⁷Florida International University, Miami, Florida 33199

¹⁸Florida State University, Tallahassee, Florida 32306

¹⁹INFN, Sezione di Ferrara, 44100 Ferrara, Italy

²⁰INFN, Laboratori Nazionali di Frascati, 00044 Frascati, Italy

²¹INFN, Sezione di Genova, 16146 Genova, Italy

²²INFN, Sezione di Roma Tor Vergata, 00133 Rome, Italy

²³INFN, Sezione di Torino, 10125 Torino, Italy

²⁴Institut de Physique Nucléaire, CNRS/IN2P3 and Université Paris Sud, Orsay, France

²⁵Institute of Theoretical and Experimental Physics, Moscow, 117259, Russia

²⁶James Madison University, Harrisonburg, Virginia 22807

²⁷Kyungpook National University, Daegu 41566, Republic of Korea

²⁸Mississippi State University, Mississippi State, MS 39762-5167

²⁹University of New Hampshire, Durham, New Hampshire 03824-3568

³⁰Nuclear Research Centre Negev, Beer-Sheva, Israel

³¹Norfolk State University, Norfolk, Virginia 23504

³²Ohio University, Athens, Ohio 45701

³³Rensselaer Polytechnic Institute, Troy, New York 12180-3590

³⁴Università di Roma Tor Vergata, 00133 Rome Italy

³⁵Skobeltsyn Institute of Nuclear Physics, Lomonosov Moscow State University, 119234 Moscow, Russia

³⁶University of South Carolina, Columbia, South Carolina 29208

³⁷Temple University, Philadelphia, PA 19122

³⁸Thomas Jefferson National Accelerator Facility, Newport News, Virginia 23606

³⁹Edinburgh University, Edinburgh EH9 3JZ, United Kingdom

⁴⁰University of Glasgow, Glasgow G12 8QQ, United Kingdom

⁴¹Virginia Tech, Blacksburg, Virginia 24061-0435

⁴²University of Virginia, Charlottesville, Virginia 22901

⁴³College of William and Mary, Williamsburg, Virginia 23187-8795

⁴⁴Yerevan Physics Institute, 375036 Yerevan, Armenia

⁴⁵Institute for Nuclear Studies, Department of Physics, The George Washington University, Washington DC 20052, USA

Short-Range Correlated (SRC) nucleon pairs are a vital part of the nucleus, accounting for almost all nucleons with momentum greater than the Fermi momentum (k_F). A fundamental characteristic of SRC pairs is having small center-of-mass (c.m.) and large relative momenta as compared to k_F , which indicates a small separation distance between the nucleons in the pair. Determining the c.m. momentum distribution of SRC pairs is essential for understanding their formation process. We report here on the extraction of the c.m. motion of proton-proton (pp) SRC pairs in Carbon and, for the first time in heavier and asymmetric nuclei: aluminum, iron, and lead, from measurements of the $A(e, e'pp)$ reaction. We find that the pair c.m. motion for these nuclei can be described by a three-dimensional Gaussian with a narrow width ranging from 140 to 170 MeV/c, approximately consistent with the sum of two mean-field nucleon momenta. Comparison with calculations appears to show that the SRC pairs are formed from mean-field nucleons in specific quantum states. The extracted c.m. widths are linearly correlated with the relative number of SRC pairs, further evidence for the selectivity of SRC pair formation.

PACS numbers:

The atomic nucleus is a complex, strongly interacting, many body system. Effective theories can successfully describe the long-range part of the nuclear many-body wave function. However, the exact description of its short-range part is still challenging. This difficulty is due to the complexity of the nucleon-nucleon (NN) interaction and the large nuclear density, which make it difficult to simplify the problem using scale-separated approaches.

Recent experimental studies have shown that approximately 20% of the nucleons in the nucleus belong to strongly interacting, momentary, short-range correlated (SRC) nucleon pairs [1–4]. These pairs are predominantly proton-neutron pairs with large relative momentum, p_{rel} , and low center-of-mass (c.m.) momentum, $p_{c.m.}$ (where high and low are relative to the nuclear Fermi momentum, k_F) [5–10]. They account for almost all of the nucleons in the nucleus with momentum greater than k_F and for most of the kinetic energy carried by nucleons in the nucleus. See Refs. [11–13] for recent reviews. SRC pairs are thus a vital part of nuclei with implications for many important topics including the possible modification of bound nucleon structure and the extraction of the free neutron structure function [11, 14–18], neutrino-nucleus interactions and neutrino oscillation experiments [19–24], neutrino-less double beta decay searches [25, 26], as well as neutron star structure and the nuclear symmetry energy [27–29].

The low c.m. momentum and high relative momentum of SRC pairs are fundamental characteristics of such pairs, and are essential indications that the nucleons in the pair are in close proximity with limited interaction with the surrounding nuclear environment [30].

Modern calculations [31] indicate that SRC pairs are temporary fluctuations due to the short-range part of the NN interaction acting on two nucleons occupying shell-model (“mean-field”) states. The exact parentage and formation process of SRC pairs is still not well understood. While state-of-the-art many-body calculations of one- and two-body momentum densities in nuclei [32–34] seem to produce SRC features that are generally consistent with measurements, they do not offer direct insight into the effective mechanisms of SRC pair formation.

Effective calculations using scale-separated approaches agree with many-body calculations [30, 35–37], suggesting that, at high-momenta, the momentum distribution of SRC pairs can be factorized into the c.m. and relative momentum distributions ,

$$n_{SRC}(\vec{p}_1, \vec{p}_2) \approx n_{c.m.}^A(\vec{p}_{c.m.}) n_{rel}^{NN}(\vec{p}_{rel}). \quad (1)$$

This implies that the relative momentum distribution of SRC pairs, $n_{rel}^{NN}(\vec{p}_{rel})$, is a universal function of the short-range part of the (NN) interaction, such that the many-body nuclear dynamics affect only the c.m. momentum distribution, $n_{c.m.}^A(\vec{p}_{c.m.})$. Therefore, extracting the c.m. momentum distribution of SRC pairs can provide valuable insight into their formation process.

The c.m. momentum distributions of SRC pairs in ${}^4\text{He}$ and C have been extracted previously from $A(e, e'pN)$ and $A(p, 2pn)$ measurements [5, 7, 9]. Here we present the first study of the c.m. momentum distribution of pp SRC pairs in nuclei heavier than C using the $A(e, e'pp)$ reaction. The cross-section for this ($e, e'pp$) two-nucleon knockout reaction approximately factorizes as a kinematic factor times the elementary electron-proton cross

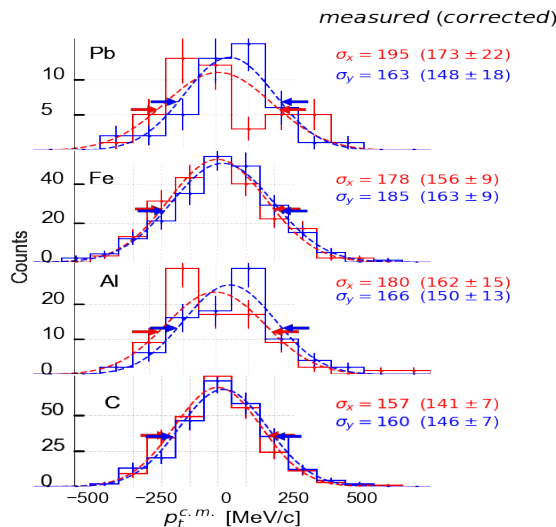


FIG. 1: (color online) The number of $A(e, e'pp)$ events plotted versus the components of $\vec{p}_{c.m.}$ perpendicular to \vec{p}_{miss} . The red and blue histograms show the \hat{x} and \hat{y} directions, respectively. The data are shown before corrections for the CLAS detector acceptance. The dashed lines show the results of Gaussian fits to the data. The widths in parentheses with uncertainties are corrected for the CLAS acceptance as discussed in the text.

section times the nuclear decay function, which defines the combined probability of finding the knocked-out nucleon pair with given energies and momenta [6, 31, 38–40]. The decay function also factorizes into relative and c.m. parts, just like Eq. 1 [6]. Therefore, the $A(e, e'pp)$ cross section is proportional to the c.m. momentum distributions of SRC pairs [6, 31, 40–42]:

$$\sigma(e, e'pp) \propto n_{c.m.}^A(\vec{p}_{c.m.}). \quad (2)$$

To increase sensitivity to the initial state properties of pp -SRC pairs, the measurement was done using high energy electrons scattering at large momentum transfer (hard scattering), in kinematics dominated by the hard breakup of SRC pairs, as discussed in detail in [11]. As discussed below, in this kinematics, Eq. 2 is a good approximation since rescattering of the two outgoing nucleons does not distort the width of the momentum distribution.

The data presented here were collected as part of the EG2 run period that took place in 2004 in Hall B of the Thomas Jefferson National Accelerator Facility (Jefferson Lab). The experiment used a 5.014 GeV electron beam, impinging on ^2H and natural C, Al, Fe, and Pb targets at the CEBAF Large Acceptance Spectrometer (CLAS) [43]. The analysis was carried out as part of the Jefferson Lab Hall B Data-Mining project.

CLAS used a toroidal magnetic field and six independent sets of drift chambers for charged particle tracking, time-of-flight scintillation counters for hadron identification, and Čerenkov counters and electro-magnetic

calorimeters for electron/pion separation. The polar angular acceptance was $8^\circ \leq \theta \leq 140^\circ$ and the azimuthal angular acceptance ranged from 50% at small polar angles to 80% at larger polar angles. See Refs. [10, 44] for details on the electron and proton identification and momentum reconstruction procedures.

The EG2 run period used a specially designed target setup, consisting of an approximately 2-cm LD_2 cryotarget followed by one of six independently-insertable solid targets (thin Al, thick Al, Sn, C, Fe, and Pb, all with natural isotopic abundance, ranging between 0.16 and 0.38 g/cm²), see Ref. [45] for details. The LD_2 target cell and the inserted solid target were separated by about 4 cm. The few-mm vertex reconstruction resolution of CLAS for both electrons and protons was sufficient to unambiguously separate particles originating in the cryotarget and the solid target.

The identification of exclusive $A(e, e'pp)$ events, dominated by scattering off $2N$ -SRC pairs, was done in two stages: (1) selection of $A(e, e'p)$ events in which the electron predominantly interacts with a single proton belonging to an SRC pair in the nucleus [8, 10, 44], and (2) selection of $A(e, e'pp)$ events by requiring the detection of a second, recoil proton in coincidence with the $A(e, e'p)$ reaction.

We selected $A(e, e'p)$ events in which the knocked-out proton predominantly belonged to an SRC pair by requiring a large Bjorken scaling parameter $x_B = Q^2/(2m_p\omega) \geq 1.2$ (where $Q^2 = \vec{q}^2 - \omega^2$, \vec{q} and ω are the three-momentum and energy, respectively, transferred to the nucleus and m_p is the proton mass). This requirement also suppressed the effect of inelastic reaction mechanisms (e.g., pion and resonance production) and resulted in $Q^2 \geq 1.4$ GeV² [7, 46]. We also required large missing momentum $300 \leq |\vec{p}_{miss}| \leq 600$ MeV/c, where $\vec{p}_{miss} = \vec{p}_p - \vec{q}$ with \vec{p}_p the measured proton momentum. We further suppressed contributions from inelastic excitations of the struck nucleon by limiting the reconstructed missing mass of the two-nucleon system $m_{miss} = [(\omega + 2m - E_p)^2 - p_{miss}^2]^{1/2} \leq 1.1$ GeV/c² (where E_p is the total energy of the leading proton). We identified events where the leading proton absorbed the transferred momentum by requiring that its momentum \vec{p}_p was within 25° of \vec{q} and that $0.60 \leq |\vec{p}_p|/|\vec{q}| \leq 0.96$ [10, 44]. As shown by previous experimental and theoretical studies, these conditions enhance the contribution of scattering off nucleons in SRC pairs and suppress contribution from competing effects [46–53].

$A(e, e'pp)$ events were selected by requiring that the $A(e, e'p)$ event had a second, recoil proton with momentum $|\vec{p}_{recoil}| \geq 350$ MeV/c. There were no events in which the recoil proton passed the leading proton selection cuts described above. The recoil proton was emitted opposite to \vec{p}_{miss} [10], consistent with the measured pairs have large relative momentum and small c.m. momentum.

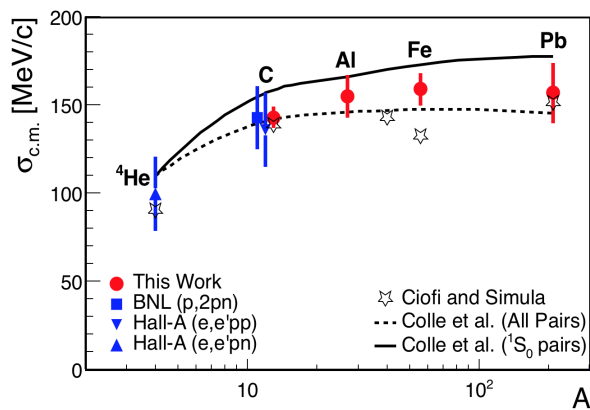


FIG. 2: (color online) The nuclear mass dependence of the one-dimensional width of the c.m. momentum distribution. The data points obtained in this work (red full circles) are compared to previous measurements (blue full squares and triangles) [5, 7, 9] and theoretical calculations by Ciofi and Simula (open stars) [54], and Colle et al., considering all mean-field nucleon pairs (dashed line) and only 1S_0 pairs (solid line) [31]. See text for details.

In the Plane Wave Impulse Approximation (PWIA), where the nucleons do not rescatter as they leave the nucleus, \vec{p}_{miss} and \vec{p}_{recoil} are equal to the initial momenta of the two protons in the nucleus before the interaction. In that case we can write

$$\vec{p}_{c.m.} = \vec{p}_{miss} + \vec{p}_{recoil} = \vec{p}_p - \vec{q} + \vec{p}_{recoil} \quad (3)$$

$$\vec{p}_{rel} = \frac{1}{2}(\vec{p}_{miss} - \vec{p}_{recoil}). \quad (4)$$

We use a coordinate system where \hat{z} is parallel to \hat{p}_{miss} , and \hat{x} and \hat{y} are transverse to it and defined by: $\hat{y} \parallel \vec{q} \times \vec{p}_{miss}$ and $\hat{x} = \hat{y} \times \hat{z}$.

Figure 1 shows the number of $A(e, e'pp)$ events plotted versus the x - and y -components of $\vec{p}_{c.m.}$ (see Eq. 3). The data shown are not corrected for the CLAS acceptance and resolution effects. As the $A(e, e'pp)$ cross section is proportional to $n_{c.m.}^A(\vec{p}_{c.m.})$, we can extract the width of $n_{c.m.}^A(\vec{p}_{c.m.})$ from the widths of the measured distributions. Both $p_{c.m.}^x$ and $p_{c.m.}^y$ are observed to be normally distributed around zero for all nuclei. Thus, as expected, $n_{c.m.}^A(\vec{p}_{c.m.})$ can be approximated by a three-dimensional Gaussian [5, 7, 9, 31, 54], and we characterize its width using σ_x and σ_y , the standard deviation of the Gaussian fits in the two directions transverse to \vec{p}_{miss} . We average σ_x and σ_y for each nucleus to get $\sigma_{c.m.}$, the Gaussian width of one dimension of $n_{c.m.}^A(\vec{p}_{c.m.})$. These widths are independent of the magnitude of p_{miss} , supporting the factorization of Eq. 3.

There are three main effects that complicate the interpretation of the raw (directly extracted) c.m. momentum distribution parameters (i.e., $\sigma_{c.m.}$): (1) kinematical offsets of the c.m. momentum in the \hat{p}_{miss} direction, (2) reaction mechanism effects, and (3) detector acceptance

and resolution effects. We next explain how each effect is accounted for in the data analysis.

(1) Kinematical offsets in the c.m. momentum direction: Since the relative momentum distribution of pairs falls rapidly for increasing $|\vec{p}_{rel}|$, it is more likely for an event with a large nucleon momentum (\vec{p}_{miss}) to be the result of a pair with smaller \vec{p}_{rel} and a $\vec{p}_{c.m.}$ oriented in the direction of the nucleon momentum. This kinematical effect will manifest as a shift in the mean of the c.m. momentum distribution in the \hat{p}_{miss} (nucleon initial momentum) direction. To isolate this effect, we worked in a reference frame in which $\hat{z} \parallel \hat{p}_{miss}$ and \hat{x} and \hat{y} are perpendicular to \hat{p}_{miss} . The extracted c.m. momentum distributions in the \hat{x} and \hat{y} directions were observed to be independent of \vec{p}_{miss} , as expected.

(2) Reaction mechanism effects: These include mainly contributions from meson-exchange currents (MECs), isobar configurations (ICs), and rescattering of the outgoing nucleons (final-state interactions or FSI) that can mimic the signature of SRC pair breakup and/or distort the measured distributions [47–49].

This measurement was performed at an average Q^2 of about 2.1 GeV^2 and $x_B \geq 1.2$ to minimize the contribution of MEC and IC relative to SRC breakup [46, 50–52]. Nucleons leaving the nucleus can be effectively “absorbed”, where they scatter inelastically or out of the phase-space of accepted events. The probability of absorption ranges from about 0.5 for C to 0.8 for Pb [44, 55–58]. Nucleons that rescatter by smaller amounts are still detected, but have their momenta changed. This rescattering includes both rescattering of the struck nucleon from its correlated partner and from the other $A - 2$ nucleons. Elastic rescattering of the struck nucleon from its correlated partner will change each of their momenta by equal and opposite amounts, but will not change $\vec{p}_{c.m.}$ (see Eq. 3) [46, 52]. To minimize the effects of rescattering from the other $A - 2$ nucleons, not leading to absorption, we selected largely anti-parallel kinematics, where \vec{p}_{miss} has a large component antiparallel to \vec{q} [46]. Relativistic Glauber calculations show that, under these conditions, FSI are largely confined to within the nucleons of the pair [46, 52, 53].

The probability of the struck nucleon rescattering from the $A - 2$ nucleons is expected to increase with A . Such rescattering, when not leading to reduction of the measured flux (i.e., absorption), should broaden the extracted c.m. momentum distribution. The measured widths do not increase strongly with A . This provides evidence that, in the kinematics of this measurement, FSI with the $A - 2$ nucleons do not distort the shape of the measured c.m. momentum distribution, in agreement with theoretical calculations [46, 52, 53].

(3) Detector acceptance and resolution effects: While CLAS has a large acceptance, it is not complete, and the measured c.m. momentum distributions need to be corrected for any detector related distortions. Following

previous analyses [7–9], we corrected for the CLAS acceptance in a 6-stage process: (1) We modeled the c.m. momentum distribution as a three-dimensional Gaussian, parametrized by a width and a mean in each direction. In the directions transverse to \hat{p}_{miss} the widths were assumed to be constant and equal to each other ($\sigma_x = \sigma_y = \sigma_t$) and the means were fixed at zero. In the direction parallel to \hat{p}_{miss} , both the mean and the width were varied over a wide range. (2) For a given set of parameters characterizing the c.m. momentum distribution in step (1), we generated a synthetic sample of $A(e, e'pp)$ events by performing multiple selections of a random event from the measured $A(e, e'p)$ events and a random $\vec{p}_{c.m.}$ from the 3D Gaussian. The combination of the two produced a sample of recoil protons with momentum ($\vec{p}_{recoil} = \vec{p}_{c.m.} - \vec{p}_{miss}$). (3) We determined the probability of detecting each recoil proton using GSIM, the GEANT3-based CLAS simulation [59]. (4) We analyzed the Monte Carlo events in the same way as the data to extract the c.m. momentum distributions and fit those distributions in the directions transverse to \hat{p}_{miss} with a Gaussian to determine their reconstructed width. (5) We repeated steps (1) to (4) using different input parameters for the 3D Gaussian model used in step (1) and obtained a ‘reconstructed’ σ_t for each set of input parameters. σ_t was varied between 0 and 300 MeV/c. The mean and width in the \hat{p}_{miss} direction were sampled for each nucleus from a Gaussian distribution centered around the experimentally measured values with a nucleus dependent width (1σ) ranging from 45 to 125 MeV/c for the mean and 30 to 90 MeV/c for the width. The exact value of the width of the distribution is a function of the measurement uncertainty for each nucleus. It extends far beyond the expected effect of the CLAS acceptance. (6) We examined the distribution of the generated vs. reconstructed widths in the directions transverse to \hat{p}_{miss} to determine the impact of the CLAS acceptance on the measured values.

The net effect of the acceptance corrections was to reduce the widths of the c.m. momentum distributions by 15–20 MeV/c for each nucleus and to increase the uncertainties.

As a sensitivity study for the acceptance correction procedure, we examined two additional variations to the event generator in the \hat{p}_{miss} direction: (A) a constant width of 70 MeV/c and (B) a width and mean that varied as a linear function of $|p_{miss}|$. The variation among the results obtained using each method was significantly smaller than the measurement uncertainties and gives a systematic uncertainty of 7%. We also performed a ‘closure’ test where we input pseudo-data with known width and statistics that matched the measurements, passed it through the CLAS acceptance to see the variation in the ‘measured’ width and then applied the acceptance correction to successfully retrieve the generated value.

The CLAS reconstruction resolution, σ_{res} , for the c.m.

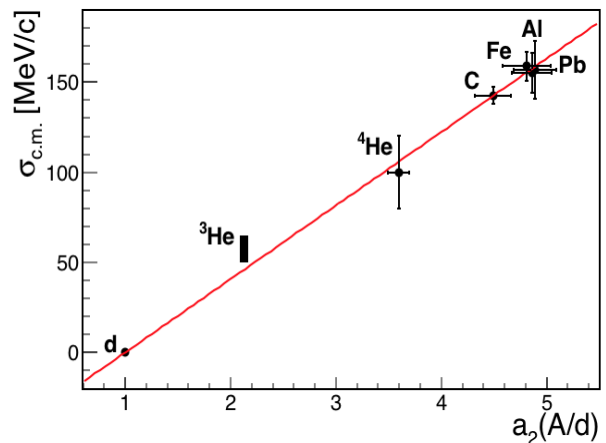


FIG. 3: The width of the c.m. momentum distribution ($\sigma_{c.m.}$) plotted versus the relative number of SRC pairs in nuclei (a_2). The a_2 values are taken from Ref. [15], based on inclusive electron scattering measurements [1–4]. The $\sigma_{c.m.}$ value for C is the weighted average of the three measurements shown in Fig. 2 and for ${}^3\text{He}$ it is taken from p - d cluster calculations [32, 33]. The deuteron has $p_{cm} = 0$ and $a_2 = 1$ by definition.

momentum of pp pairs was measured using the exclusive $d(e, e'\pi^-pp)$ reaction and was found to equal 20 MeV/c. We subtracted this in quadrature from the measured c.m. width: $\sigma_{corrected}^2 = \sigma_{measured}^2 - \sigma_{res}^2$, which amounts to a small, 2–3 MeV/c, correction.

Figure 2 shows the extracted $\sigma_{c.m.} = \sigma_t$, in the directions transverse to \hat{p}_{miss} , including acceptance corrections and subtraction of the CLAS resolution. The uncertainty includes both statistical uncertainties as well as systematic uncertainties due to the acceptance correction procedure.

The extracted value of $\sigma_{c.m.}$ for C is consistent with previous C($e, e'pp$) measurements of $\sigma_{c.m.}^{pp}$ [7] and C(p, ppn) measurements of $\sigma_{c.m.}^{pn}$ [5], with significantly reduced uncertainty. The extracted width grows very little from C to Pb, and is consistent with a constant value within uncertainties (i.e., it saturates). The saturation of $\sigma_{c.m.}$ with A supports the claim that, in the chosen kinematics, FSI with the $A - 2$ nucleons primarily reduces the measured flux, while not significantly distorting the shape of the extracted c.m. momentum distribution.

Figure 2 also shows a comparison of the data to three theoretical calculations [31, 54]. The calculations are based on a mean-field approach for the c.m. motion of the parent nucleons that create the SRC pairs. The overall agreement of the data with the calculations support the theoretical picture of SRC pairs being formed from temporal fluctuations of mean-field nucleons [11]. The theoretical predictions do differ in the types of parent mean-field nucleon pairs included in the calculation. In the approach of Ref. [54] all pairs are considered, while Ref. [31] shows the results for all pairs as well as for nu-

cleons in a relative 1S_0 state [60, 61]. The width of the $\vec{p}_{c.m.}$ distribution is about 20% larger for the 1S_0 pairs. The experimentally extracted widths are systematically higher than the calculations considering all pairs, indicating some selectivity, but are somewhat lower than the 1S_0 calculation that represents the most restrictive conditions on the mean-field nucleons that form SRC pairs [31].

We note that the SRC-pair c.m. momentum distributions extracted from experiment differ from those extracted directly from ab-initio calculations of the two-nucleon momentum distribution. The latter are formed by summing over *all* two-nucleon combinations in the nucleus and therefore include contributions from non-SRC pairs. See discussion in Ref. [30].

In an attempt to gain a little more understanding of how these pairs might be formed, we examined a possible connection between $\sigma_{c.m.}$ and a_2 , the relative number of SRC pairs in nuclei [1–4, 11, 15] (see Fig. 3). a_2 is dominated by pn -SRC pairs. While $\sigma_{c.m.}$ was extracted primarily from measurements of pp -SRC pairs, it should be the same for both pp and np pairs [31].

The linear correlation observed in Fig. 3 is intriguing. $\sigma_{c.m.}$ describes the width of the SRC pairs momentum distribution, while $a_2(A/d)$ describes its magnitude (i.e. the abundance of SRC pairs) [11]. Given that there is no clear theoretical argument relating the two, the linear correlation between these two seemingly independent properties is somewhat surprising. Naively, the probability that a nucleon belongs to a correlated pair in the nucleus should be proportional to the number of its nearest neighbors, implying that $a_2 \propto \rho$, where ρ is the nuclear density. Similarly, if SRC pairs result from two mean-field nucleons fluctuating into an SRC pair, then the width of their $\vec{p}_{c.m.}$ distribution should be proportional to the typical nuclear fermi momenta, so that $\sigma_{c.m.} \propto k_F \propto \rho^{1/3}$. However, this apparent contradiction could be resolved if the parent nucleons of SRC pairs need to be in a specific quantum state, such as a relative 1S_0 state. In that case the width of their momentum distribution would increase faster, see the calculations in Fig. 2.

As the width of the c.m. momentum distribution is calculable within mean-field approaches, understanding the origin of this linear relationship could lead to new insight to the formation process of SRC pairs and the interplay between single-body and many-body dynamics in nuclear systems.

In conclusion, we report the extraction of the width of the c.m. momentum distribution, $\sigma_{c.m.}$, for pp -SRC pairs from $A(e, e'pp)$ measurements in C, Al, Fe, and Pb. The new data is consistent with previous measurements of the width of the c.m. momentum distribution for both pp and pn pairs in C. $\sigma_{c.m.}$ increases very slowly and might even saturate from C to Pb, supporting the claim that final state interactions are negligible between the two outgoing nucleons and the residual $A - 2$ nucleus. The com-

parison with theoretical models supports the claim that SRC pairs are formed from mean-field pairs in specific quantum states. However, improved measurements and calculations are required to determine the exact states. Lastly, we find a linear correlation between the width of the momentum distribution, $\sigma_{c.m.}$, and its magnitude, the relative number of SRC pairs measured in different nuclei, which also implies that SRC pair formation is selective.

We acknowledge the efforts of the staff of the Accelerator and Physics Divisions at Jefferson Lab that made this experiment possible. We are also grateful for many fruitful discussions with L.L. Frankfurt, M. Strikman, J. Ryckebusch, W. Cosyn, M. Sargsyan, and C. Ciofi degli Atti. The analysis presented here was carried out as part of the Jefferson Lab Hall B Data-Mining project supported by the U.S. Department of Energy (DOE). The research was supported also by the National Science Foundation, the Israel Science Foundation, the Chilean Comisin Nacional de Investigacin Cientfica y Tecnolgica, the French Centre National de la Recherche Scientifique and Commissariat l'Energie Atomique the French-American Cultural Exchange, the Italian Istituto Nazionale di Fisica Nucleare, the National Research Foundation of Korea, and the UKs Science and Technology Facilities Council. Jefferson Science Associates operates the Thomas Jefferson National Accelerator Facility for the DOE, Office of Science, Office of Nuclear Physics under contract DE-AC05-06OR23177. The raw data from this experiment are archived in Jefferson Labs mass storage silo. E. O. Cohen would like to acknowledge the Azrieli Foundation.

* Contact Author hen@mit.edu

† On sabbatical leave from Nuclear Research Centre Negev, Beer-Sheva, Israel

‡ Current address: Idaho State University, Pocatello, Idaho 83209

- [1] L. Frankfurt, M. Strikman, D. Day, and M. Sargsyan, Phys. Rev. C **48**, 2451 (1993).
- [2] K. Egiyan et al. (CLAS Collaboration), Phys. Rev. C **68**, 014313 (2003).
- [3] K. Egiyan et al. (CLAS Collaboration), Phys. Rev. Lett. **96**, 082501 (2006).
- [4] N. Fomin et al., Phys. Rev. Lett. **108**, 092502 (2012).
- [5] A. Tang et al., Phys. Rev. Lett. **90**, 042301 (2003).
- [6] E. Piassetzky, M. Sargsian, L. Frankfurt, M. Strikman, and J. W. Watson, Phys. Rev. Lett. **97**, 162504 (2006).
- [7] R. Shneor et al., Phys. Rev. Lett. **99**, 072501 (2007).
- [8] R. Subedi et al., Science **320**, 1476 (2008).
- [9] I. Korover, N. Muangma, O. Hen, et al., Phys.Rev.Lett. **113**, 022501 (2014).
- [10] O. Hen et al. (CLAS Collaboration), Science **346**, 614 (2014).
- [11] O. Hen, G. A. Miller, E. Piassetzky, and L. B. Weinstein, Rev. Mod. Phys. **89**, 045002 (2017).

- [12] C. Ciofi degli Atti, Phys. Rept. **590**, 1 (2015).
- [13] L. Frankfurt, M. Sargsian, and M. Strikman, International Journal of Modern Physics A **23**, 2991 (2008).
- [14] L. B. Weinstein, E. Piasetzky, D. W. Higinbotham, J. Gomez, O. Hen, and R. Shneur, Phys. Rev. Lett. **106**, 052301 (2011).
- [15] O. Hen, E. Piasetzky, and L. B. Weinstein, Phys. Rev. C **85**, 047301 (2012).
- [16] O. Hen, D. W. Higinbotham, G. A. Miller, E. Piasetzky, and L. B. Weinstein, Int. J. Mod. Phys. **E22**, 1330017 (2013).
- [17] O. Hen, A. Accardi, W. Melnitchouk, and E. Piasetzky, Phys. Rev. D **84**, 117501 (2011).
- [18] J.-W. Chen, W. Detmold, J. E. Lynn, and A. Schwenk, Phys. Rev. Lett. **119**, 262502 (2017).
- [19] H. Gallagher, G. Garvey, and G. P. Zeller, Ann. Rev. Nucl. Part. Sci. **61**, 355 (2011).
- [20] L. Fields et al. (MINERvA Collaboration), Phys. Rev. Lett. **111**, 022501 (2013).
- [21] G. A. Fiorentini et al. (MINERvA Collaboration), Phys. Rev. Lett. **111**, 022502 (2013).
- [22] R. Acciarri et al., Phys. Rev. D **90**, 012008 (2014).
- [23] L. B. Weinstein, O. Hen, and E. Piasetzky, Phys. Rev. **C94**, 045501 (2016).
- [24] T. Van Cuyck, N. Jachowicz, R. Gonzalez-Jimenez, M. Martini, V. Pandey, J. Ryckebusch, and N. Van Dessel, Phys. Rev. **C94**, 024611 (2016).
- [25] M. Kortelainen, O. Civitarese, J. Suhonen, and J. Toivanen, Physics Letters B **647**, 128 (2007).
- [26] L. S. Song, J. M. Yao, P. Ring, and J. Meng, Phys. Rev. **C95**, 024305 (2017).
- [27] O. Hen, B.-A. Li, W.-J. Guo, L. B. Weinstein, and E. Piasetzky, Phys. Rev. C **91**, 025803 (2015).
- [28] B.-J. Cai and B.-A. Li, Phys. Rev. **C93**, 014619 (2016).
- [29] O. Hen, A. W. Steiner, E. Piasetzky, and L. B. Weinstein (2016), 1608.00487.
- [30] R. Weiss, R. Cruz-Torres, N. Barnea, E. Piasetzky, and O. Hen, Phys. Lett. B **780**, 211 (2018).
- [31] C. Colle, W. Cosyn, J. Ryckebusch, and M. Vanhalst, Phys. Rev. **C89**, 024603 (2014).
- [32] R. B. Wiringa, R. Schiavilla, S. C. Pieper, and J. Carlson, Phys. Rev. C **89**, 024305 (2014).
- [33] J. Carlson, S. Gandolfi, F. Pederiva, S. C. Pieper, R. Schiavilla, K. E. Schmidt, and R. B. Wiringa, Rev. Mod. Phys. **87**, 1067 (2015).
- [34] T. Neff, H. Feldmeier, and W. Horiuchi, Phys. Rev. C **92**, 024003 (2015).
- [35] J. Ryckebusch, M. Vanhalst, and W. Cosyn, Journal of Physics G: Nuclear and Particle Physics **42**, 055104 (2015).
- [36] M. Alvioli, C. Ciofi degli Atti, and H. Morita, Phys. Rev. **C94**, 044309 (2016).
- [37] C. Ciofi degli Atti, C. B. Mezzetti, and H. Morita, Phys. Rev. **C95**, 044327 (2017).
- [38] L. L. Frankfurt and M. I. Strikman, Phys. Rep. **76**, 215 (1981).
- [39] L. Frankfurt and M. Strikman, Phys. Rep. **160**, 235 (1988).
- [40] J. Ryckebusch, Phys. Lett. **B383**, 1 (1996), nucl-th/9605043.
- [41] C. Ciofi degli Atti, S. Simula, L. Frankfurt, and M. Strikman, Phys. Rev. C **44**, R7 (1991).
- [42] M. M. Sargsian, T. V. Abrahamyan, M. I. Strikman, and L. L. Frankfurt, Phys. Rev. C **71**, 044615 (2005).
- [43] B. A. Mecking et al., Nucl. Instrum. Meth. **A503**, 513 (2003).
- [44] O. Hen et al. (CLAS Collaboration), Phys. Lett. **B722**, 63 (2013).
- [45] H. Hakobyan et al., Nucl. Instrum. Meth. **A592**, 218 (2008).
- [46] L. L. Frankfurt, M. M. Sargsian, and M. I. Strikman, Phys. Rev. **C56**, 1124 (1997).
- [47] D. Groep et al., Phys. Rev. C **63**, 014005 (2000).
- [48] K. I. Blomqvist et al., Phys. Lett. **B421**, 71 (1998).
- [49] L. J. H. M. Kester et al., Phys. Rev. Lett. **74**, 1712 (1995).
- [50] R. G. Arnold et al., Phys. Rev. **C42**, 1 (1990).
- [51] J. M. Laget, Phys. Lett. **B199**, 493 (1987).
- [52] C. Colle, W. Cosyn, and J. Ryckebusch, Phys. Rev. **C93**, 034608 (2016).
- [53] M. M. Sargsian, Int. J. Mod. Phys. **E10**, 405 (2001).
- [54] C. Ciofi degli Atti and S. Simula, Phys. Rev. C **53**, 1689 (1996).
- [55] G. Garino et al., Phys. Rev. C **45**, 780 (1992).
- [56] T. O'Neill, W. Lorenzon, P. Anthony, R. Arnold, J. Arrington, E. Beise, J. Belz, P. Bosted, H.-J. Bulten, M. Chapman, et al., Physics Letters B **351**, 87 (1995), ISSN 0370-2693.
- [57] D. Abbott, A. Ahmidouch, T. A. Amatuni, C. Armstrong, J. Arrington, K. A. Assamagan, K. Bailey, O. K. Baker, S. Barrow, K. Beard, et al., Phys. Rev. Lett. **80**, 5072 (1998).
- [58] K. Garrow, D. McKee, A. Ahmidouch, C. S. Armstrong, J. Arrington, R. Asaturyan, S. Avery, O. K. Baker, D. H. Beck, H. P. Blok, et al., Phys. Rev. C **66**, 044613 (2002).
- [59] M. Holtrop, *Clas - geant simulation*, URL http://nuclear.unh.edu/~maurik/gsim_info.shtml.
- [60] M. Vanhalst, W. Cosyn, and J. Ryckebusch, Phys. Rev. **C84**, 031302 (2011).
- [61] M. Vanhalst, J. Ryckebusch, and W. Cosyn, Phys. Rev. C **86**, 044619 (2012).